ELEMENTAL CHEMISTRY OF FUGITIVE DUST FROM QUARRIES AND ASSOCIATED SITES

M. Fowler[1], H.E. Datson[2,3] and W.B. Williams[1,2]

[1] *School of Earth and Environmental Sciences, University of Portsmouth, Burnaby Building, Burnaby Road, Portsmouth, PO1 3QL.*

[2] *DustScan Ltd., Griffin House, Market Street, Charlbury, Oxfordshire, OX7 3PJ.*

[3] *Energy and Resources Research Institute, School of Process, Environmental and Materials Engineering, University of Leeds, Leeds, LS2 9JT.*

Abstract

Fugitive dust from quarrying and related extractive industry activities is a long-standing and intractable problem. Attempts to control emissions are directed by legislation and informed by statutory guidance, within the overall context of national and international air quality strategies. In many cases, local monitoring is a prerequisite for efficient development of dust suppression. In cases of dispute or of particular concern, it is often necessary to confidently attribute problem dust to one or more local source(s) – in effect to answer the fundamental question: whose dust is it? This contribution describes a method of dust source attribution developed by DustScan Ltd, which combines a simple and cost-effective technique for collecting ambient dust by direction, with multi-element analysis by plasma spectrometry.

DustScan is a passive system for monitoring fugitive dust 360° around a replaceable sampling head. It uses a transparent, permanent adhesive, 'sticky pad' on a 70 mm diameter cylindrical monitoring head. Measurement of dust coverage on the sticky pads after monitoring uses a computer-based scanning system and bespoke software. The pattern of dusting on the sticky pad indicates the direction and scale of potential dust nuisance by direction. Given this information, samples may be taken according to suspected dust source, and subjected to a range of geochemical analyses including acid dissolution (HF-HNO_3) prior to analysis by ICPAES or ICP-MS. Rigorous blank correction procedures are essential to account for metallic components of the sticky pads themselves, but good results are obtained for a range of elements including Cu, As, Cd and Pb. Careful assessment of the data often allows source-specific elemental criteria to be established; the elemental fingerprints of dust type. In the simplest of cases, this is sufficient to identify the source of a problem dust, but more commonly some form of mixture deconvolution is required. Various intuitive graphical techniques have been successful in small-scale studies, but multivariate statistics and least-squares mass balance methods provide powerful tools for source attribution as the site database increases. Examples of the application of such techniques to a variety of extractive industry sites demonstrate the utility of the methods in the extractive industries and elsewhere.

Fowler, M., Datson, H.E. and Williams, W.B., 2011. Elemental chemistry of fugitive dusts from quarries and associated sites. Pp. 146-159 in Hunger, E. and Walton, G. (Eds.)
Proceedings of the 16th Extractive Industry Geology Conference, EIG Conferences Ltd, 194pp.

e-mail: mike.fowler@port.ac.uk

Introduction

By its very nature, the non-petroleum extractive industry produces airborne particulates (dust) as a result of day-to-day activities. Within the industry dust might be considered an inevitable consequence of operation, but in the outside world there is growing intolerance of adverse environmental impacts. In this respect, air quality is of national and local significance (DEFRA, 2000, 2007). Regulatory controls are becoming more stringent, with the onus increasingly on the operator to undertake routine monitoring of environmental control measures. Consequently, considerable expense and effort are often required to minimise propagation of fugitive dust into the nearby environment. However, there are usually many sources of ambient dust, not all of which are related to site operations or even the site itself. This often causes local tension and occasionally leads to litigation, which rapidly escalates the funding required. A key question in any resulting discussion is "*whose dust is it?*".

Source attribution of airborne particulates has a number of academic and more practical applications, from the global (e.g. tracing trans-boundary pollutants over intercontinental distances), and regional (e.g. understanding of the causes of smog in large conurbations such as Beijing and Mexico City), to the more local but nonetheless important (e.g. investigating the health effects of road traffic dust inhalation and assisting in local disputes about the environmental impact of an industry). In many such studies, collection of dust samples and subsequent chemical analysis is critical, providing quantitative data for comparison with potential source materials. A wide range of modern instrumental analytical techniques has been applied to such work, including Gas Chromatography-Mass Spectrometry (GC-MS) for the identification of polycyclic aromatic hydrocarbons, Inductively-Coupled Plasma Mass Spectrometry (ICP-MS) for the analysis of metals, Scanning Electron Microscopy (SEM) for high-power magnification and imaging, laser-ablation ICP-MS for isotopic applications such as tracing the origins of anthropogenic Pb, and very many more.

Applications to "nuisance" dust have been relatively few, and the chemistry of industrial nuisance dust is therefore poorly known. This is partly a result of research (rightly) concentrating on dust fractions to which health-related affects have been attributed (e.g. COMEAP, 2001, 2009), and partly because of a severe lack of clarity in the definition of both nuisance dust itself and the nuisance that it causes.

The resulting plethora of monitoring methods and procedures (e.g. QUARG, 1996; Environment Agency, 2004) has done little to facilitate the type of source attribution work that is sometimes required: it is often erroneously assumed that all nuisance dust in the vicinity of an industrial site is caused by that site. In this paper, a procedure is described by which fugitive nuisance dust can be confidently attributed to source, and given appropriate sampling arrangements the proportion of site dust can be quantified in local samples. It refines the methods described in Datson & Fowler (2007) and Fowler *et al.* (2010), and applies them to a range of extractive industry sites in order to demonstrate their utility to this industrial sector, and to begin a much-needed database of background chemical information. The approach adopted is typical of the relatively new discipline "environmental forensics", which uses rigorous environmental science within the appropriate legislative and regulatory framework.

Methodology

The approach adopted in this study combines a simple, directional passive sampling device (DustScan D100) with sophisticated metals analysis (ICP-MS), following straightforward dust dissolution (HF-HNO_3 attack). The result is a diverse dataset of complementary information that can be used in a number of ways to address dust source attribution and related issues (optimisation of dust suppression, monitoring of specific pollutants, informing standard operating procedures (SOPs), compliance monitoring and environmental performance monitoring).

These dust samplers are widely used at minerals sites to assess dust flux (e.g. Walton and Datson, 2010). The dust monitoring head is mounted on a stand and fixed approximately 2 m from the ground. The sticky pads are manufactured by specialist suppliers from stock material and comprise three principal layers: a transparent PVC film, a permanent, cross-linked polymer acrylic adhesive and a silicone-coated paper liner that is removed at the start of monitoring. Samples are normally taken over weekly or fortnightly intervals then sealed, scanned and, as illustrated in Figure 1, are analysed with bespoke computer software to report percentage Absolute Area Coverage (%AAC) and percentage Effective Area Coverage (%EAC) at 15° intervals (Datson and Birch, 2006). Precise directional control enables sub-samples to be selected according either to selected directions of interest (e.g. on pathways between suspected source/s and receptor/s) or according to directional dust level (*e.g.* where AAC > 80%).

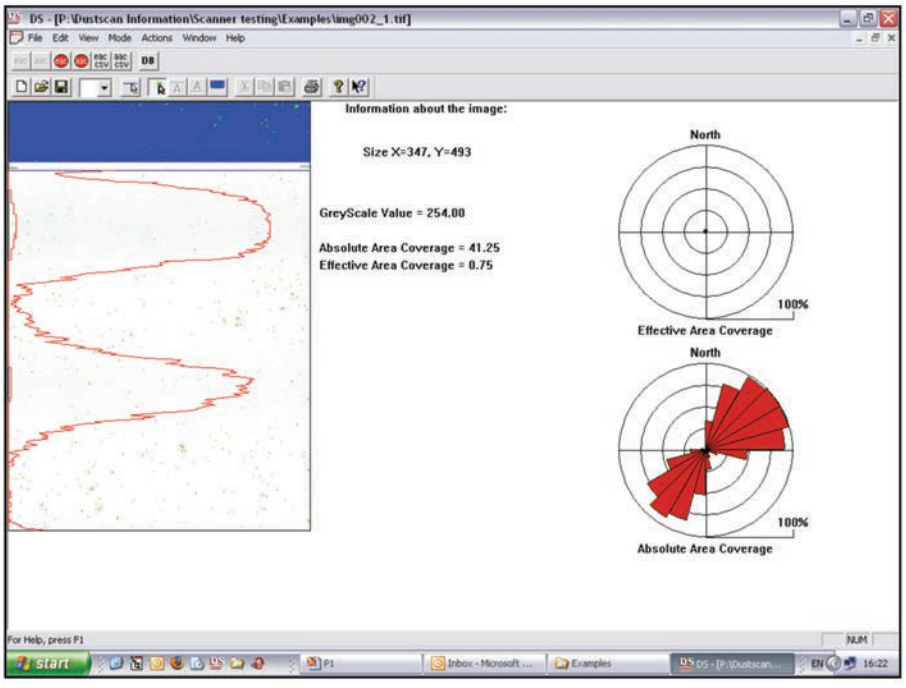

Figure 1. *DustScan bespoke scanning methodology, showing the AAC and EAC results of one scan depicted on the stick pad itself (left) and as directional rose diagrams (right).*

Sub-samples of the sealed sticky pads can be taken from any part of the collected dust, but routinely a 15° segment (ca. 9mm wide) that is 80 mm long is excised, at directions selected according to the criteria outlined above. Depending on dusting density, this provides sufficient dust for a reliable analysis and allows a sensible archive sample to be retained. A "reference" strip of the same size is taken from an unexposed part of *each* sticky pad, to provide data for blank correction. This has been discussed in detail by Datson and Fowler (2007), and is necessary because of the sometimes-significant and often variable metals content of the plastics and adhesives used in the sticky pads themselves. Thus, at present, each analysis requires two sub-samples – one of the dust and an accompanying blank taken from the reference area. These are cut into smaller pieces (to facilitate acid ingress) and placed into clean 25 ml Teflon beakers. In an appropriate fume hood, 3 ml of trace metal grade HF and 3 ml of trace metal grade HNO_3 are added to each. The beakers are placed on a hotplate and allowed to stand at room temperature overnight. The acids are gently evaporated the following morning, to incipient dryness. A further 3 ml aliquot of HNO_3 is added subsequently, and evaporated to dryness. The resulting solids are taken into solution to a final volume of 20 ml of 2.5% HNO_3. Approximately 10 ml of this solution is transferred to a 15 ml centrifuge tube, to be stored in a refrigerator until analysis.

The ICP-MS at the University of Portsmouth is an Agilent 7500ce. For this purpose, the octopole collision cell is run in He mode, and Rh is used as an internal standard at 25 ppb. The instrument is calibrated for a selection of major and trace metals, using dilutions of a Merck® multi-element calibration solution appropriate to the expected concentration ranges of the metals to be analysed. Data quality for the method is routinely monitored using specially-prepared sticky pads loaded with powdered CRMs – NIST 2710 (Montana contaminated soil) and USGS SCo-1 (Cody shale). These are then sub-sampled as above and subjected to the entire dissolution process. Accuracy and precision are estimated to be better than 20% for most elements (Datson and Fowler, 2007; Fowler *et al*, 2010), and example equiline plots for batches analysed in this study are shown in Figure 2. The main advantages of ICP-MS are its rapid, multi-element capability and very low instrumental detection limits for most elements (parts per billion (ppb) and below). *Method* detection limits have been estimated (Datson and Fowler, 2007) in the order of

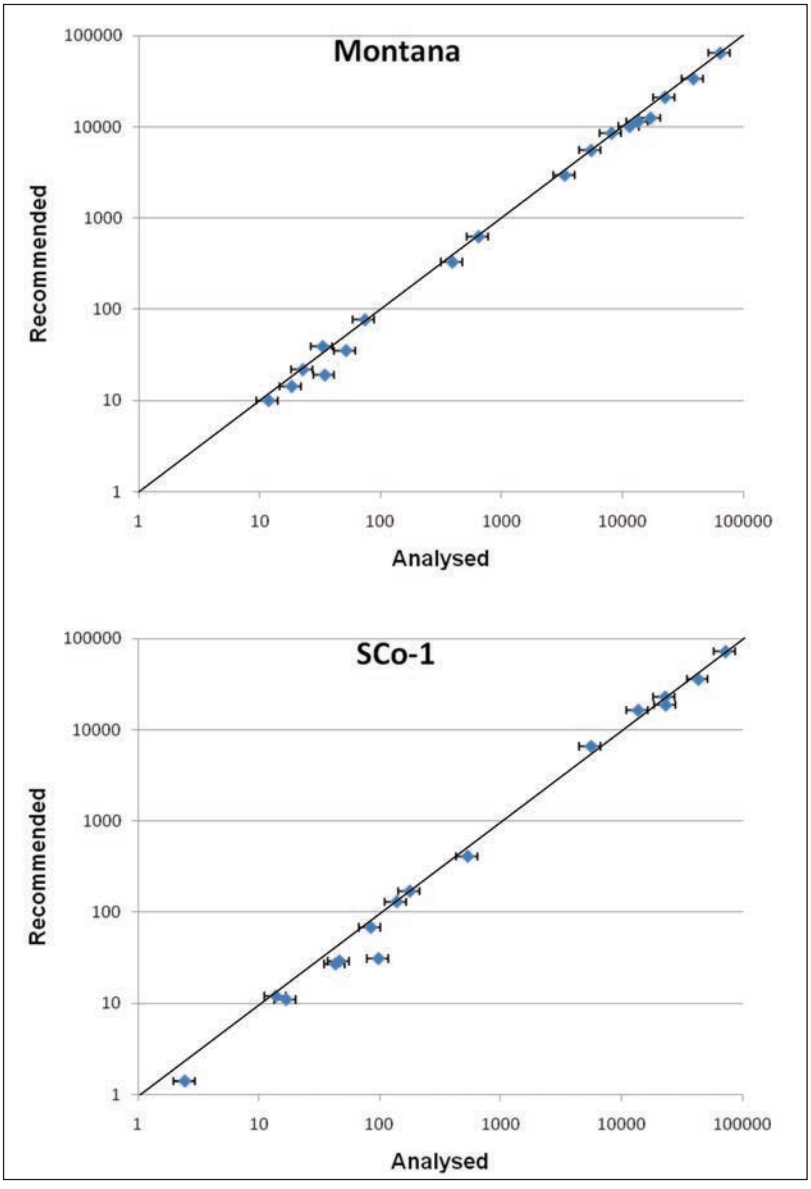

Figure 2. *Examples of reference materials analysed alongside samples for this study. Error bars are ± 20%.*

a few parts per million (ppm) for major elements (Na, K, Mg, Ca, Al, Fe, Mn) and a few ppb for trace metals bar Ba and Zn. The latter are limited by their content and variability in the sticky pad materials, as noted above, and are currently not analysed.

Sampling rationale

For this contribution, samples from a selection of extractive industry sites at which dust monitoring has been undertaken in the recent past were recovered from an archive of direction dust samples. The sites will not be identified for reasons of confidentiality, but they include the following generic types: hard rock quarries, sand and gravel extraction, surface coal mines, secondary aggregates, land remediation and mineral stockpiles (Plate 1). Table 1 sets out details of the samples analysed; it shows the predominant lithology at each site. The sub-samples were selected according to dust coverage (as AAC%).

Plate 1. *A composite image showing 6 of the mineral sites used in this investigation. Top left: surface coal mine, Yorkshire. Top right: Jurassic limestone quarry, Oxfordshire. Centre left: Dolerite quarry, Cornwall. Centre right: Carboniferous limestone quarry, Wiltshire. Bottom left: (Jurassic) river terrace sand and gravel. Bottom right: land remediation.*

		Predominant mineral/site type	Directional arc analysed	AAC%	Sample end date	Sampling duration (days)
Sample reference	00663	Sand and gravel	255-270	100	21/08/03	7
	00665	Sand and gravel	255-270	100	09/10/03	7
	00667	Sand and gravel	255-270	100	09/10/03	7
	00669	Sand and gravel	255-270	100	10/06/04	14
	00671	Sand and gravel	255-270	100	18/06/04	8
	00673	Limestone	255-270	100	10/10/05	14
	00674	Limestone	255-270	100	26/09/05	14
	00675	Limestone	315-330	98	09/10/06	30
	00677	Limestone	195-210	100	07/09/05	35
	00679	Limestone	195-210	100	21/12/04	27
	00681	Granite	210-225	98	08/09/06	13
	00683	Granite	210-225	100	27/07/06	15
	00685	Chalk	165-180	100	19/12/06	77
	00687	Chalk	045-060	100	05/04/07	61
	00689	Chalk	240-255	100	18/12/06	17
	00691	Chalk	240-255	100	11/01/07	24
	00693	Limestone	030-045	100	14/05/07	14
	00695	Limestone	030-045	100	29/05/07	15
	00697	Dolomite	240-255	99	16/08/07	7
	00699	Dolomite	195-210	100	16/08/07	7
	00701	Sand and gravel	000-015	79	21/09/07	7
	00703	Sand and gravel	165-180	80	21/09/07	7
	00705	Limestone	240-255	100	04/09/07	7
	00707	Limestone	240-255	100	25/09/07	7
	00709	Surface coal	090-105	100	23/10/03	7
	00711	Surface coal	090-105	100	06/11/03	7
	00713	Limestone	315-330	100	28/03/08	21
	00715	Limestone	090-105	100	12/05/08	6
	00717	Limestone	315-330	100	09/06/08	7
	00719	Land remediation	075-090	100	13/03/08	7
	00721	Land remediation	075-090	100	03/04/08	7
	00723	Land remediation	075-090	100	28/02/08	7
	00725	2^{y} aggregates	000-015	100	03/06/08	29
	00727	2^{y} aggregates	000-015	100	02/07/08	30
	00729	2^{y} aggregates	000-015	100	28/07/08	28
	00731	Granite	000-015	100	05/09/08	7
	00733	Granite	000-015	100	02/10/08	15
	00735	Dolerite	225-240	100	03/09/08	30
	00737	Dolerite	165-180	100	03/09/08	30
	00740	Marine sand/fly ash	000-015	38	10/03/08	4
	00742	Marine sand/fly ash	330-345	20	10/03/08	4
	00743	Marine sand/fly ash	000-015	20	10/03/08	4
	00745	Marine sand/fly ash	180-195	65	10/03/08	4
	00746	Marine sand/fly ash	345-360	24	10/03/08	4
	00748	Marine sand/fly ash	180-195	50	10/03/08	4
	00750	Marine sand/fly ash	330-345	21	17/03/08	5
	00752	Marine sand/fly ash	345-360	25	17/03/08	5

Table 1. *Sample details, lithology and dust coverage (AAC %).*

RESULTS AND DATA HANDLING

ICP-MS analytical data and DustScan dusting intensity parameters are presented in Table 2, as ppm in solution after appropriate blank correction and total content of the analysed elements in µg. Initial perusal of the data illustrates the range in dust coverage (AAC from 21% to 100%), reflected in the variable total element content (4 µg to ca. 3000 µg). As would be expected from crustal element averages, in the majority of the samples Al, K, Ca and Fe are the most abundant metals (Si was not analysed since it is lost during the acid digestion), with others present at rather lower abundance, sometimes below the method detection limit.

It is always difficult (often impossible) to sufficiently interrogate a tabulated dataset that contains a significant number of analyses, and some more advanced form of data handling is usually needed. The methods chosen depend on the nature of the data and the type of information required from the exercise. Experience has shown that for the purposes of dust source attribution, multi-element diagrams organised to provide elemental "fingerprints" of specific dust types are very useful. These depend on pre-existing knowledge with which to select the samples to differentiate. A less judgemental approach uses multivariate statistics, for which no preconceptions are required. Both approaches are adopted below in order to characterise the extractive industry dusts and demonstrate the potential of the methods used.

Crustal enrichment factors are commonly used in the airborne particulates literature as a way of summarising the overall elemental chemistry of dust samples and emphasising any departures from "normal" crustal abundances. Analytical data for any given element are divided by the abundance of Al in that sample, and the derived ratio divided by the equivalent for "average

		Na	Mg	Al	K	Ca	V	Cr	Mn	Fe	Co	Ni	Cu	As	Sr	Mo	Ag	Cd	Pb	Total µg
Sample reference	00663	BDL	BDL	5.221	2.646	27.861	0.012	0.011	0.172	7.589	0.004	0.005	0.009	0.003	0.052	0.001	BDL	BDL	0.034	872.380
	00665	BDL	BDL	2.101	0.603	8.757	0.004	0.003	0.051	2.042	BDL	0.002	0.005	0.002	0.023	0.000	BDL	BDL	0.012	272.102
	00667	BDL	BDL	5.869	1.648	32.746	0.014	0.016	0.175	6.409	0.006	0.009	0.019	0.004	0.077	0.001	BDL	BDL	0.067	941.175
	00669	BDL	BDL	2.403	2.456	22.054	0.007	0.006	0.074	2.301	0.002	0.004	0.009	0.002	0.037	0.000	BDL	BDL	0.026	587.610
	00671	BDL	BDL	5.162	1.622	47.087	0.013	0.010	0.158	6.337	0.008	0.008	0.008	0.005	0.079	0.001	BDL	BDL	0.031	1210.575
	00673	BDL	BDL	1.424	BDL	BDL	0.002	0.003	0.079	1.143	BDL	0.003	BDL	0.001	BDL	0.000	BDL	BDL	0.008	53.244
	00674	1.629	1.660	7.852	2.519	3.462	0.011	0.010	0.184	4.857	BDL	0.010	0.009	0.000	0.022	0.000	BDL	BDL	0.009	444.666
	00675	BDL	BDL	BDL	1.247	8.228	0.001	BDL	0.018	0.658	0.001	BDL	BDL	BDL	0.049	0.000	BDL	BDL	0.012	204.293
	00677	BDL	BDL	2.713	1.299	0.664	0.004	0.005	0.063	2.036	0.003	0.003	0.004	0.000	0.010	0.000	BDL	BDL	0.005	136.166
	00679	BDL	BDL	2.935	1.782	0.777	0.005	0.029	0.048	1.642	BDL	0.002	BDL	BDL	0.015	BDL	BDL	0.001	0.004	144.777
	00681	BDL	BDL	BDL	BDL	0.458	BDL	BDL	0.017	0.142	0.002	BDL	BDL	0.000	BDL	BDL	BDL	BDL	0.002	12.413
	00683	BDL	BDL	BDL	BDL	0.366	BDL	BDL	0.010	2.257	BDL	BDL	BDL	0.004	0.011	0.000	BDL	BDL	0.004	53.026
	00685	BDL	BDL	BDL	BDL	BDL	0.001	BDL	0.003	0.202	0.001	BDL	BDL	BDL	0.011	0.000	BDL	BDL	0.005	4.461
	00687	BDL	BDL	1.308	0.474	8.855	0.002	0.002	0.020	0.766	0.051	0.002	0.005	BDL	0.014	0.000	BDL	BDL	0.006	230.111
	00689	2.685	BDL	1.898	2.226	6.666	0.004	0.009	0.063	2.179	0.001	0.003	0.036	0.001	0.017	0.002	BDL	BDL	0.016	316.116
	00691	BDL	BDL	1.559	2.058	4.250	0.003	0.006	0.055	2.047	0.001	0.002	0.021	0.001	BDL	0.001	BDL	BDL	0.015	200.342
	00693	BDL	BDL	1.809	0.495	1.001	0.002	BDL	0.013	0.802	0.000	BDL	BDL	0.001	BDL	BDL	BDL	BDL	0.002	82.499
	00695	BDL	BDL	BDL	BDL	BDL	BDL	BDL	0.008	2.558	BDL	BDL	BDL	BDL	BDL	BDL	BDL	BDL	BDL	51.316
	00697	BDL	BDL	5.061	2.000	13.020	0.003	0.005	0.006	0.288	0.018	0.002	0.018	0.000	0.010	BDL	BDL	BDL	0.004	408.713
	00699	BDL	30.975	2.948	BDL	59.286	0.010	0.007	0.307	2.608	0.002	0.006	0.006	0.001	0.015	0.001	BDL	0.001	0.048	1924.414
	00701	1.744	BDL	8.027	4.403	8.152	0.011	0.013	0.192	4.631	0.002	0.005	BDL	0.002	0.039	0.000	BDL	BDL	0.015	544.694
	00703	BDL	BDL	4.957	3.893	5.603	0.007	0.013	0.091	2.868	0.001	0.003	0.004	0.001	0.026	0.000	BDL	BDL	0.014	349.606
	00705	BDL	BDL	2.824	1.842	14.216	0.006	0.017	0.068	1.855	0.001	0.003	0.005	0.002	0.033	0.000	BDL	BDL	0.010	417.656
	00707	BDL	2.860	11.042	3.196	111.600	0.028	0.019	0.302	12.738	0.005	0.013	0.015	0.007	0.153	0.001	BDL	BDL	0.052	2840.628
	00709	BDL	BDL	5.753	BDL	0.920	0.009	0.006	0.099	10.121	0.004	0.012	0.012	0.002	BDL	0.001	BDL	BDL	0.019	339.154
	00711	BDL	BDL	2.863	1.102	BDL	0.005	BDL	0.014	2.752	0.016	0.005	0.012	0.001	BDL	0.001	BDL	BDL	0.011	135.637
	00713	BDL	BDL	BDL	BDL	91.328	0.002	0.002	0.067	0.418	0.001	0.003	BDL	BDL	0.068	0.000	BDL	0.001	0.021	1838.210
	00715	BDL	BDL	BDL	0.935	13.987	0.002	0.003	0.040	1.067	0.002	0.008	0.004	0.000	0.014	0.000	BDL	BDL	0.015	321.549
	00717	BDL	BDL	1.852	BDL	42.165	0.003	0.003	0.061	2.203	0.001	0.003	0.005	0.001	0.044	0.000	BDL	BDL	0.008	926.993
	00719	BDL	BDL	BDL	BDL	BDL	BDL	BDL	0.046	3.285	0.001	BDL	BDL	BDL	BDL	0.001	BDL	BDL	0.005	66.759
	00721	BDL	2.535	1.519	BDL	4.423	0.002	BDL	0.018	0.963	0.000	0.002	0.005	0.000	0.021	0.000	BDL	BDL	0.007	189.927
	00723	BDL	BDL	BDL	BDL	BDL	BDL	BDL	BDL	BDL	BDL	BDL	BDL	BDL	BDL	BDL	BDL	BDL	BDL	N/A
	00725	BDL	BDL	2.141	0.860	6.001	0.002	0.002	0.091	1.570	0.000	BDL	0.006	0.001	BDL	BDL	BDL	BDL	0.014	213.784
	00727	BDL	BDL	4.291	1.319	24.070	0.007	0.004	0.292	2.850	0.002	0.005	BDL	0.002	0.021	0.000	BDL	BDL	0.009	657.454
	00729	BDL	BDL	2.808	1.281	17.050	0.005	0.003	0.228	2.511	0.001	0.004	BDL	0.001	0.013	0.000	BDL	BDL	0.003	478.143
	00731	BDL	BDL	3.062	2.581	0.315	BDL	BDL	0.020	0.898	BDL	BDL	0.013	0.008	BDL	0.001	BDL	BDL	0.008	138.119
	00733	BDL	BDL	BDL	BDL	BDL	BDL	BDL	BDL	BDL	BDL	BDL	BDL	BDL	BDL	BDL	BDL	BDL	BDL	N/A
	00735	1.987	BDL	2.456	0.746	0.416	0.001	BDL	0.034	2.820	0.000	0.011	0.012	0.020	BDL	0.000	BDL	BDL	0.007	170.200
	00737	BDL	1.499	1.969	BDL	0.304	0.001	BDL	0.019	1.610	0.000	0.005	0.005	0.007	BDL	BDL	BDL	BDL	0.005	108.495
	00740	2.824	4.380	1.543	4.093	2.153	BDL	0.002	0.008	0.552	0.001	0.002	0.004	BDL	0.039	0.000	BDL	BDL	0.013	312.274
	00742	3.351	7.319	3.580	4.589	16.480	0.001	0.003	0.021	1.361	0.002	0.003	0.004	BDL	0.060	0.000	BDL	BDL	0.005	735.570
	00743	2.852	6.302	3.021	2.739	14.100	0.001	0.003	0.019	1.237	0.002	0.003	0.004	BDL	0.047	0.000	BDL	BDL	0.004	606.667
	00745	3.067	5.566	2.795	6.286	3.103	BDL	0.015	0.008	0.584	0.002	0.002	BDL	BDL	0.035	0.000	BDL	BDL	0.019	429.639
	00746	3.233	5.425	3.136	6.541	4.095	BDL	0.010	0.014	0.920	0.002	0.005	BDL	BDL	0.040	0.000	BDL	BDL	0.009	468.615
	00748	3.135	5.930	2.011	4.939	2.714	BDL	0.004	0.009	0.557	0.001	0.002	0.005	BDL	0.039	0.000	BDL	BDL	0.010	387.108
	00750	3.559	4.817	1.444	5.700	3.870	BDL	0.002	0.006	0.362	0.001	BDL	BDL	BDL	0.040	0.000	BDL	BDL	0.005	396.123
	00752	2.929	6.683	1.821	3.316	3.886	BDL	0.002	0.006	0.378	0.001	0.001	BDL	BDL	0.039	0.000	BDL	BDL	BDL	381.295

Table 2. *ICP-MS analytical data – ppm in solution and total mass in sample. Note: BDL; Below Detection Limit.*

crust". The results for a number of elements can then be plotted on a logarithmic, multi-element diagram such as those of Figure 3. A sample with exactly the same composition as average crust will plot as a horizontal straight line at 1.00. Elemental enrichment compared with the crustal average will plot above the line, depletion will plot below. Each sample will thus generate a line; a "fingerprint" of its elemental composition. These can then be used as an effective means of comparison.

In Figure 3, average site data have been plotted in four groups – chalk plus dolomite, dolerite plus granite, limestone plus sand and gravel plus secondary aggregates, and remediation plus marine sand plus open cast coal. Data falling below detection limit are not plotted, resulting in some gaps in the patterns. Members of the first three groups have patterns similar to each other. It is not surprising that chalk- and dolomite-associated sites show similar elemental chemistry. Both show significant major element enrichments in Ca (and K), and the dolomite site in Mg. Of the trace metals, both are enriched in Cr, Co, Cu, As and Pb, the dolomite site also in Cd. The igneous-related sites likewise show similar pattern shapes, although enrichment/depletion might vary. For example, the major element shape from Na to Ca is similar, yet (unsurprisingly) the granite site has significant depletion in Mg whereas the dolerite site does not. Interestingly, both these sites show a considerable peak at As: both are located in SW England which has well-known regional enhancement in As resulting from the historic mining activity in the area. Much of the dolerite data falls below detection limit (therefore not plotted). The third group of similar patterns includes sites related to sand and gravel extraction, secondary aggregates and (interestingly) the limestone-related site. These are characterised by major-element depletions in Na and Mg and enrichments in K and Ca. There are also significant peaks at As and Pb. Finally, the data for the marine sand site, industrial remediation and opencast coal are plotted together, for convenience rather than similarity. The marine sand site pattern is characterised by high Na, Mg, K and Sr – for obvious reasons. The industrial remediation site also has enhanced Na and Mg, but also V, Cr, Mn, Fe and Pb – common industrial metals. The opencast coal site has depleted Na, Mg and Ca but significant enrichment in Cr, Co, As and Pb – all of which is consistent with the geochemistry of coal and its host sandstones and shales. It seems, therefore, that the general geochemical character of dusts within the range of extractive industry sites considered here is a rational reflection of the site substrates and processes. This lends confidence to the suggestion that site dust might be identifiable, and indeed quantifiable, in mixtures received at local receptors. However, this "intuitive" approach might not be the most objective, in the sense that data are interpreted within the framework of preconceived ideas, albeit hopefully sensible ones.

A complementary approach with datasets such as this is to employ multivariate statistics. Figure 4 shows the loadings plot and scores plot of Principal Component

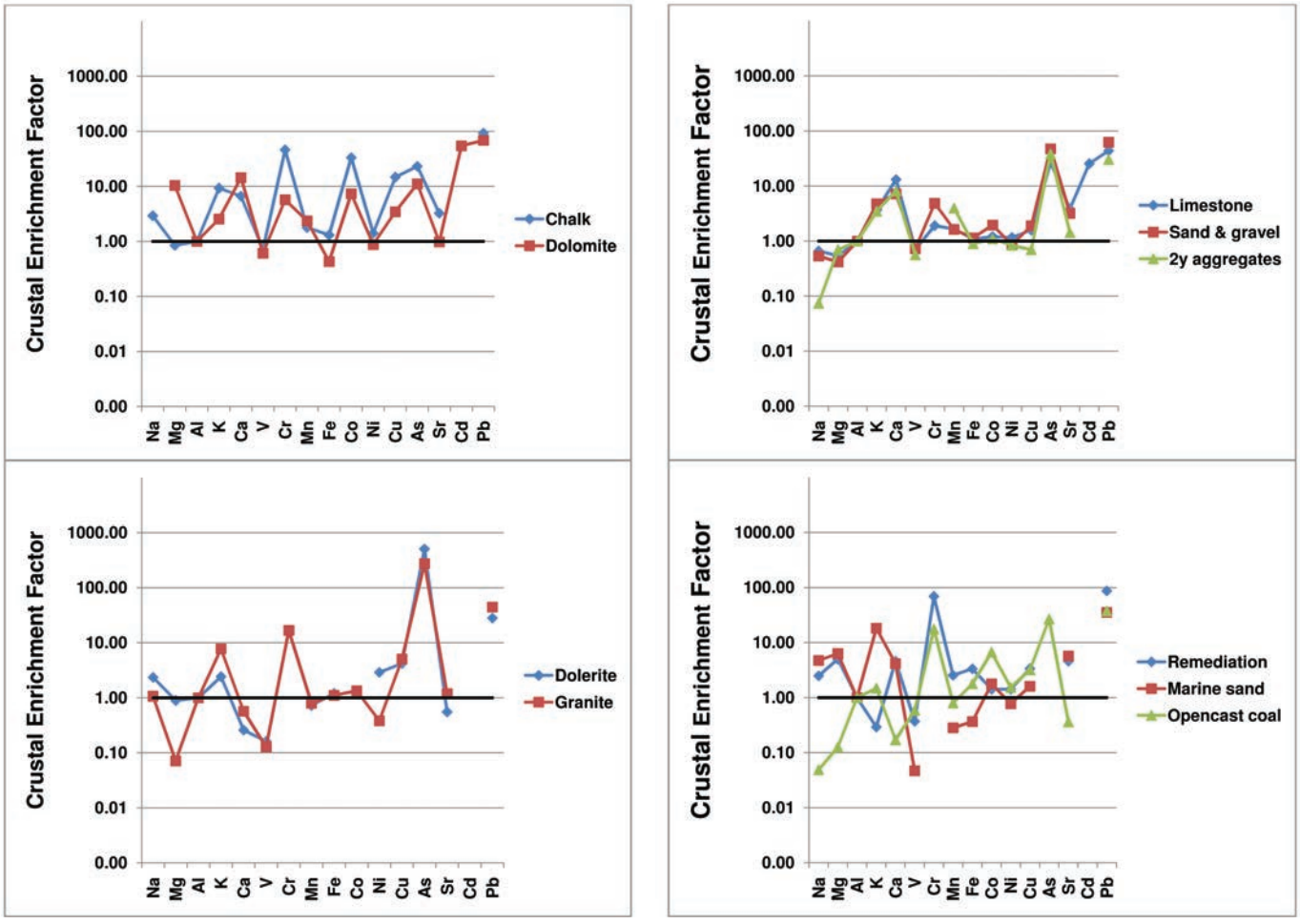

Figure3. *Elemental fingerprints of extractive industry dusts.*

Analysis (PCA) of the data used in this study. They were recast to proportions in order to avoid detection limit influence of the statistical results, and a logarithmic transformation was applied (after Fowler et al, 2010). The loadings plot summarises element groups – all except Ca are positively loaded onto principal component (pc) 1, whereas Na, Mg, K, Sr and As are positively loaded onto pc2 with the transition metals (and Cd) negatively so. The scores plot records variance from the average sample and enables any sample groups to be identified, for example the data from the marine sands site fall almost alone into the top left quadrant of the diagram. The igneous site

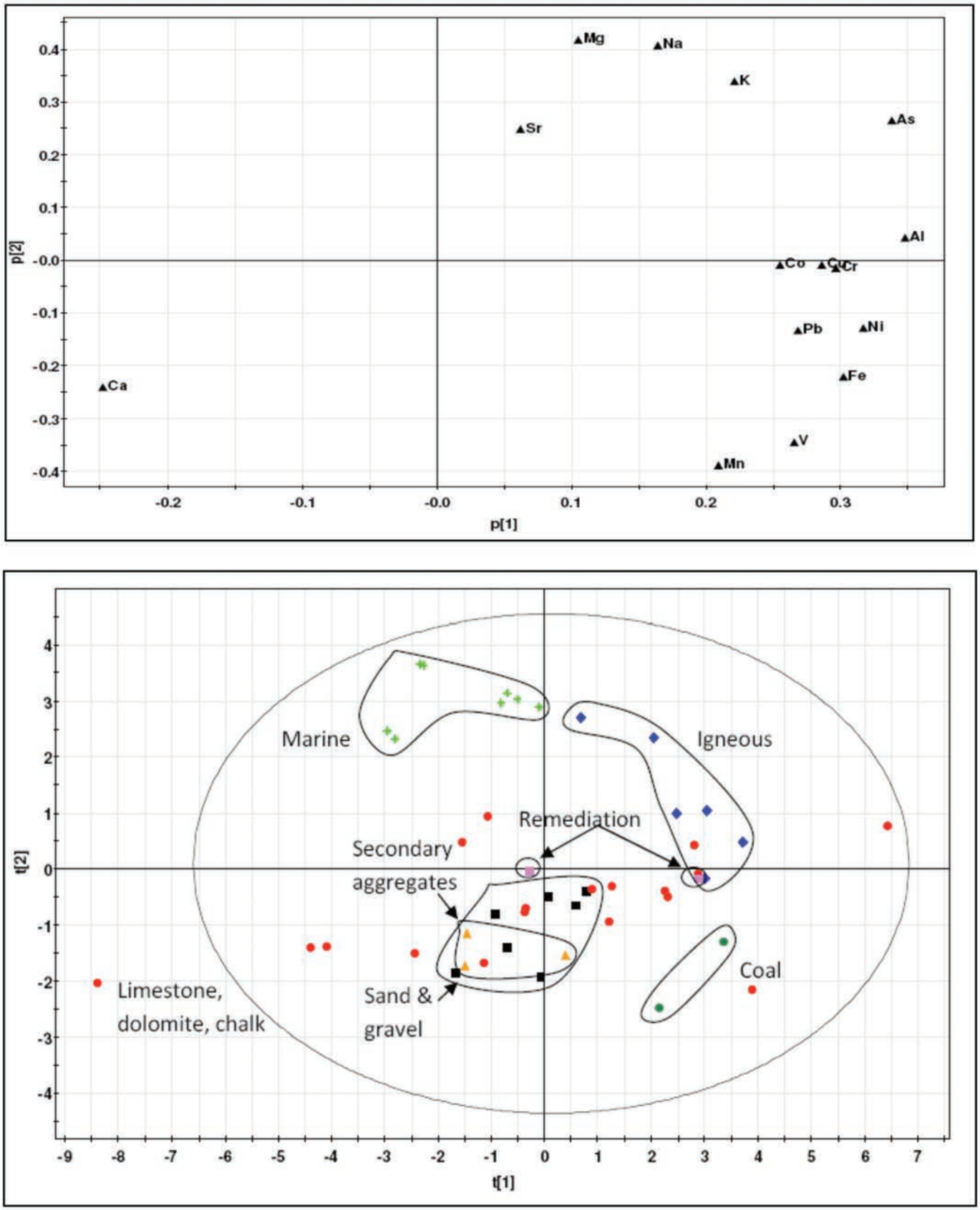

Figure 4. *Principal Component Analysis loadings (top) and scores (bottom) plots.*

samples occupy the top right quadrant. Sand and gravel and secondary aggregate sites overlap below the midline, and dust from the opencast coal site is in the lower right quadrant. Samples from the carbonate sites (limestone, dolomite and chalk) form a broad band across the plot, around the t[2] midline.

These features can be rationalised by reference to bar charts of illustrative individual samples (Figure 5), which depict elemental enrichment or depletion with respect to the average for the sample set. In general accord with the conclusions derived from the intuitive approach, the marine sands site sample has enrichment in Na, Mg, K, Ca and Sr (sea-spray?), and is depleted in transition metals and Al. The igneous site sample has high Na, Al and K (acid feldspar?), Cu and As (mineralisation?), and low Ca, V, Cr and Ni. The carbonate site sample is enriched in Ca, Mg and Mn (dolomite?) and depleted in other elements. Finally, a sample from the sand and gravel extraction site is depleted relative to average in Mg, Cu and As but enriched in Al, K, V and Mn. Thus, the completely objective statistical approach also produces sample groupings and comparative results that are explicable in terms of site character, in a reassuringly similar way to the intuitive approach outlined above.

It is therefore not unreasonable to expect that some aspects of dust chemistry might be manipulated in order to quantify the relative proportions of different dusts, especially when combined with DustScan directional information. A selection of methods with which to attempt this is presented below, using data from previous relevant published studies (Fowler et al, 2010), or commercial reports (with permission and suitably anonymised). On the basis of sample characterisation as described above, critical element ratios may be selected that stretch the data distribution between two (or more) end members (which are generally defined as "background" and "site" dust), and arithmetic binary mixing lines superimposed to provide quantitation estimates.

Each of the examples in Figure 6 has two potential source compositions (end-members of the mixing calculations - background and site-specific), several sampling locations at variable distance from site, and a number of sampling intervals each producing a data point. It is clear from both diagrams that the sample localities fall in rational, overlapping groups from which sensible site conclusions may be drawn. Further, comparison of the data distribution yields quantitative estimates of the relative proportions of the end member dusts. For example, in Figure 6 (left) the location 5 deposition dust monitor has approximately 50% of background and site dust in both sampling intervals, whereas location 1 has in excess of 90% site dust and location 3 between 10 and 20% derived from the site. Figure 6 (right) likewise shows location 1 to be dominated by site dust during three sampling intervals, while location two has only some 20% during one. Locations 3 and 4 show variable proportions, though generally in excess of 50% derived from the site.

Although this method has been successful in a number

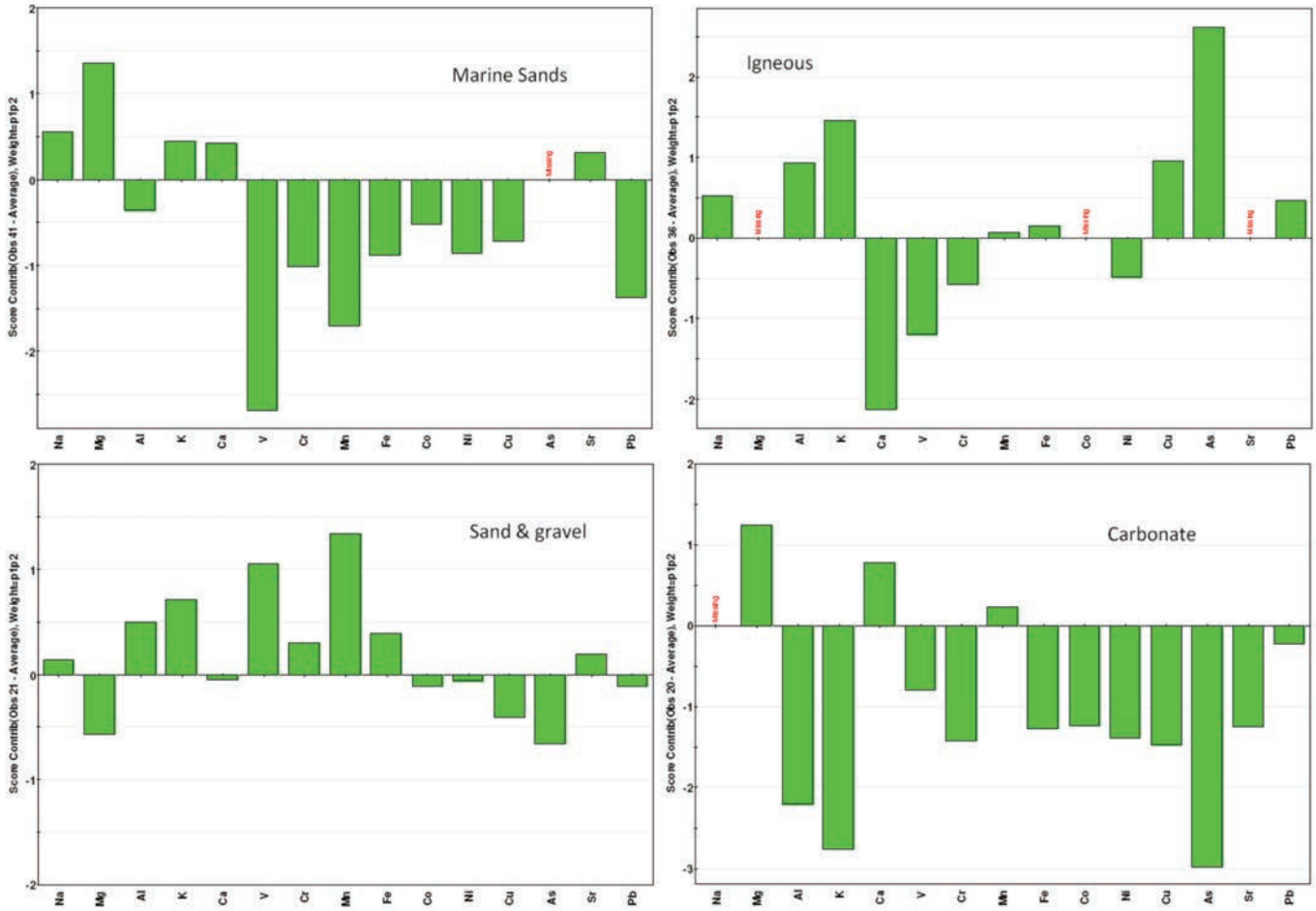

Figure 5. *Bar charts showing elemental characteristics separated by PCA.*

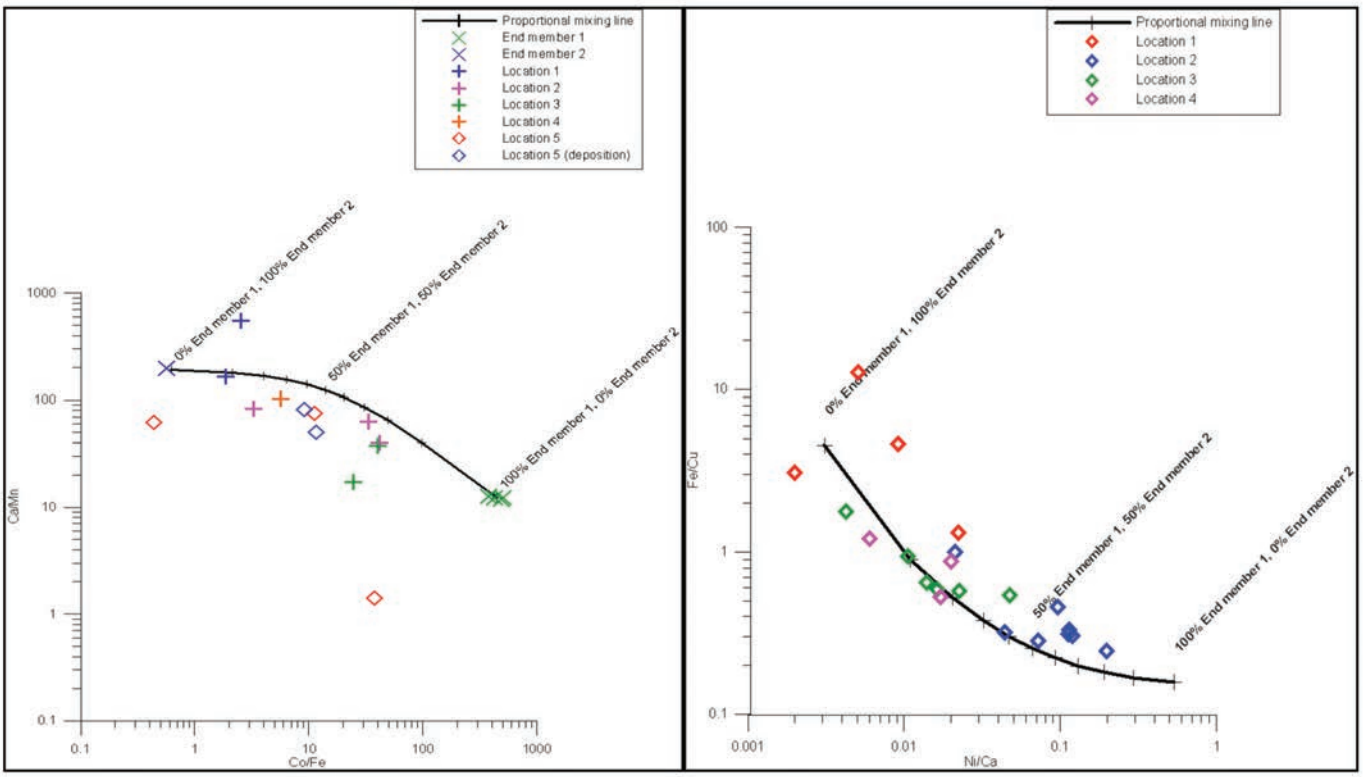

Figure 6. *Binary mixing plots of critical element ratios from two source apportionment studies.*

of studies, it uses just a fraction of the available elemental data (in these cases only four elements). A more comprehensive approach is offered by a variety of least-squares mixing programmes which provide variations on a theme of chemical mass balance. In these, iterative solutions to multi-element source mixing are provided which minimise the residual differences between sample and model. Figure 7 shows screen grabs from one such programme – CMB 8.2 distributed by the US Environmental Protection Agency, specifically designed for use with airborne particulates data. The example chosen is of a modelled three-component mixture from a landfill site which was the subject of several commercial reports. There are two background dust analyses and one "problem" dust end member. The total element concentration measured was 76.70 µg and the model has calculated a fit to 74.67 µg, by using 12.27 µg of the problem dust plus 28.77 and 33.63 µg of each of the background dusts. This has resulted in close fits for all analysed elements bar Na, for which the calculated value of 0.157 µg is a poor match for the analysed 3.329 µg. Since all other elements are so close (e.g. Al calculated has 22.582 vs. measured 22.743, Ca has 21.704 vs. 21.506, Ti has 1.087 vs. 1.053 and V has 0.027 vs. 0.029 µg), some judgement must be applied to the validity of this particular data point, or the model rejected and/or modified accordingly. The clear advantages of such programmes are the use of the whole elemental dataset and the inclusion of a number of potential source compositions. Estimates of fit are provided (R square and CHI square in CMB 8.2) which lend confidence, or otherwise, to the computed solutions. However, rigour is lost as the number of potential sources increases, such that it is possible to generate spurious good fits if care is not exercised.

The final quantitation method explored here returns to multivariate statistics, and is a technique complementary to PCA. Partial Least Squares analysis (PLS – also known as Projection to Latent Structures) again uses all the elements available, and seeks to explain the variance of a given sample within the PCA matrix by reference to a specified sample, which in this case represents one or other of the potential sources. Clearly, a good match suggests a high proportion of that source in the target sample, whereas a poor match suggests the contrary. Figure 8 shows the result of PLS on the same dataset from which the CMB 8.2 example was selected. Some 150 samples are plotted along the x-axis, and the success of the model is monitored on the y-axis – 1.0 being a perfect fit. Clearly, some samples are well explained by reference to the problem dust, while others are not. Pleasingly, those that are not are well explained by the chosen background dust, and so there is a clear antithetic relationship between the two plots. Using the figures thus generated, a quantitative estimate of problem dust proportion can be produced for each sample.

In any detailed investigation of dust source attribution, it adds considerable confidence if two or more quantitation methods provide similar results. Figure 9 shows a comparison of the three methods outlined above for one substantial dataset. Figure 9 (top) shows a binary mixing curve drawn through the data cloud, between end members of site dust and background dust. The annotated figures represent the PLS estimations derived for a selection of the data points, demonstrating low values of problem dust at one end of the binary mixing line, and uniformly high values at the other. A clear correlation is thus established. Figure 9 (bottom) shows the PLS quantitation for the same dataset plotted against CMB data, again showing a clear correlation. These plots confirm that three different methods provide similar estimations of problem dust proportion, and each lends credibility to the other.

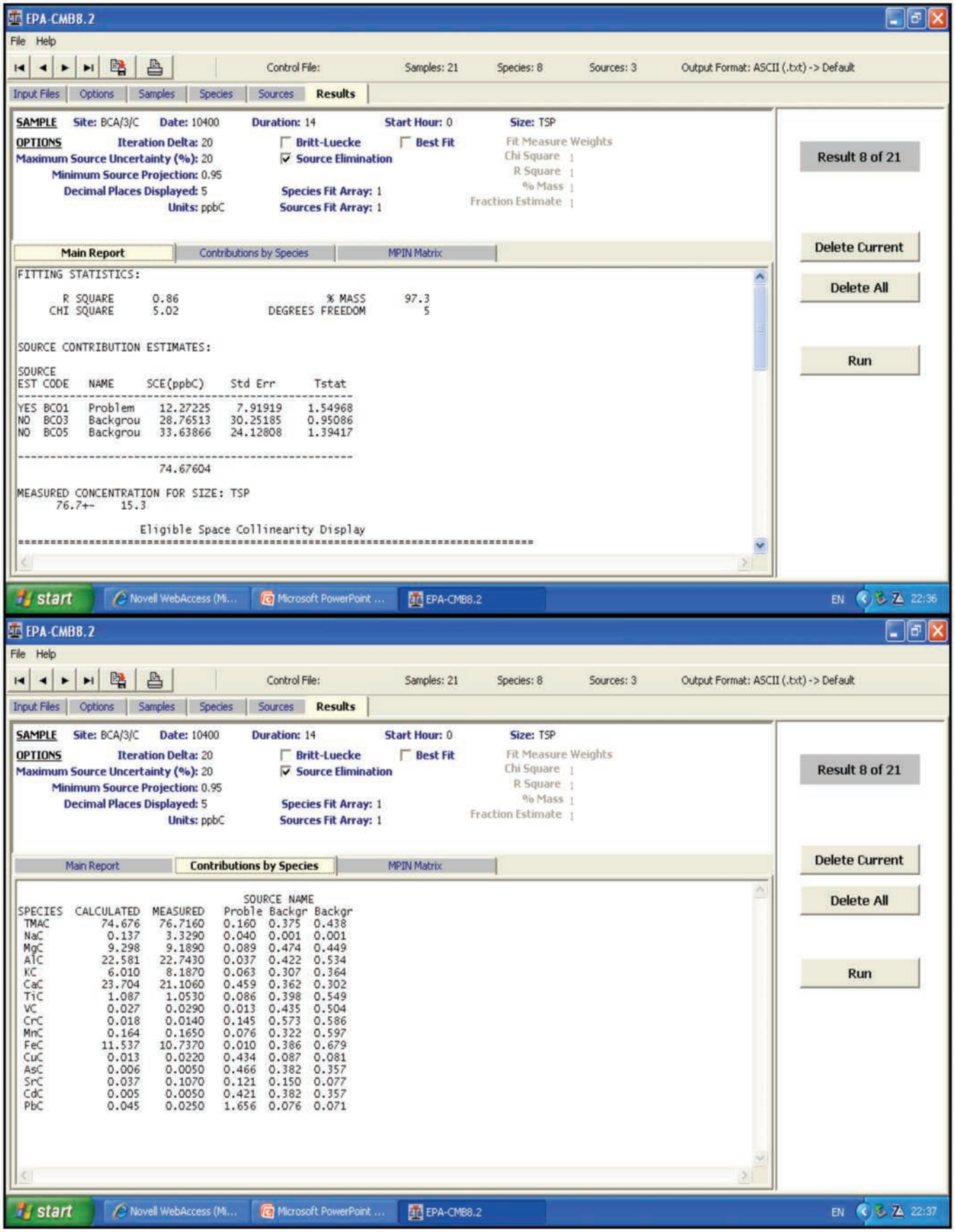

Figure 7. *Results of Chemical Mass Balance calculations for one sample from a dataset derived from an extractive industry site, using USEPA software CMB8.2.*

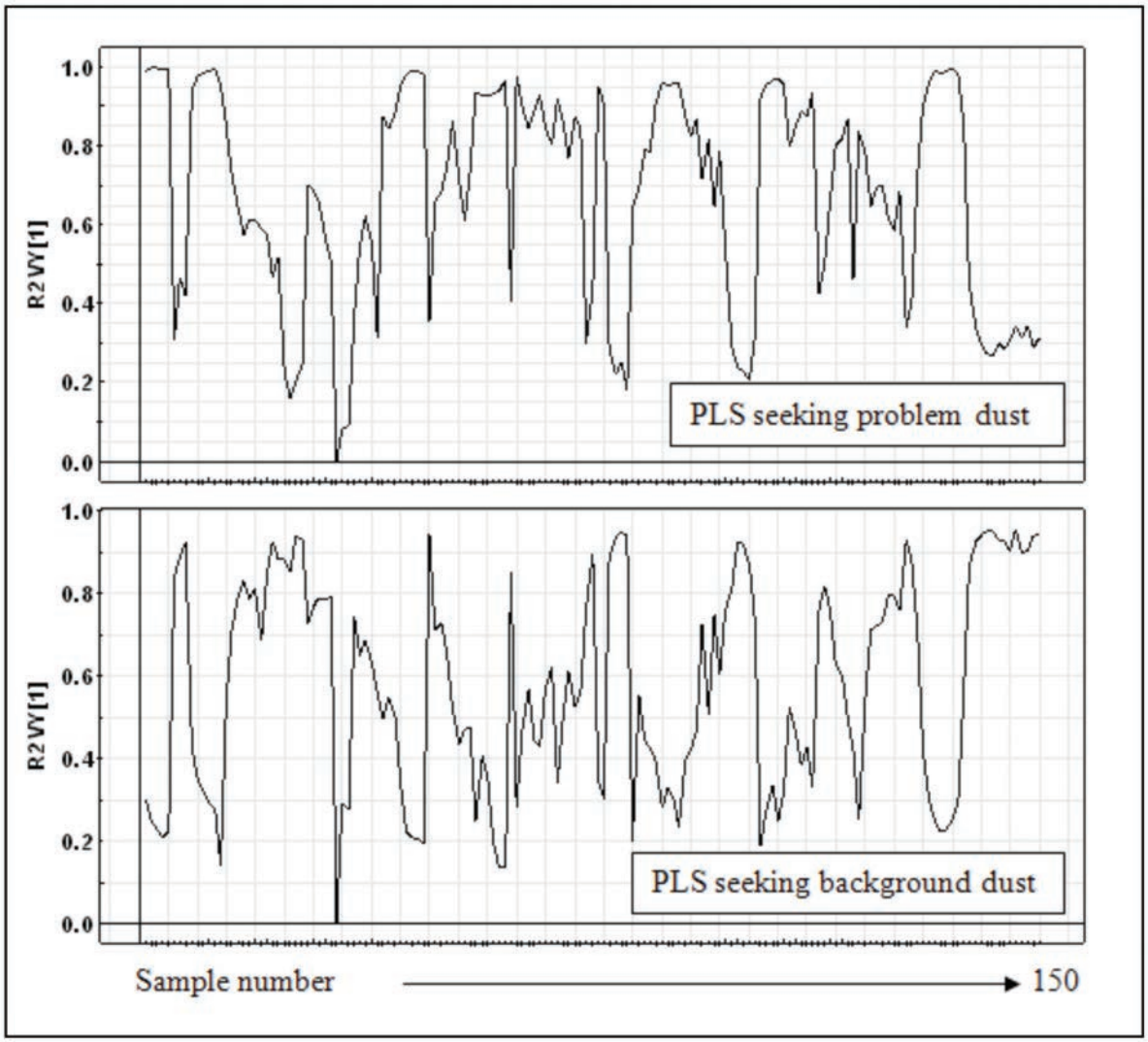

Figure 8. *Partial Least Squares analysis of a dataset using "problem" dust and background dust. Note the antithetic relationship of the plots – samples explained well by the problem dust are explained poorly by the background dust. One missing data point registers zero on both.*

Dust mapping

Once the analytical data have been transformed into a quantitative dataset by one or more of the methods outlined above, it is possible to present the data graphically in order to display periodic dust distributions. A number of software packages is available for such purposes, ISATIS being one of the more robust. ISATIS uses variography and kriging to interpolate between known data points, generating predictive data for unknown points within in a defined area relative to the sampling grid. These generated points are then plotted on a raster to produce a map.

Figure 10 shows a modified version of a fortnightly dust map generated through a calendar year study at one site. 19 DS100 passive dust monitors were deployed between the problem-dust source and potential receptors, to assess dust movement on and around the site. Based on the dataset generated by ICP-MS analysis and proportions derived from a mixing model and multivariate statistics approach as outlined above, the highest proportions of the problem dust were identified to the north and north east of the site. Local meteorological data may be used in conjunction with such maps, and in this sampling interval winds were generally from the south and south west.

Since it is easy to overlook that such maps are geostatistical models, it is important to have a way of demonstrating the error built in to the calculations. Complementary error maps allow a visual display of the standard error of the generated dataset, providing a confidence constraint when displaying data graphically. Standard error maps not only support the mapping in this way, but are a means of identifying areas within the sampling grid that would benefit from enhanced monitoring. With small datasets, the standard error of interpolations between known data points will be greater. Unfortunately, the need to sample in many

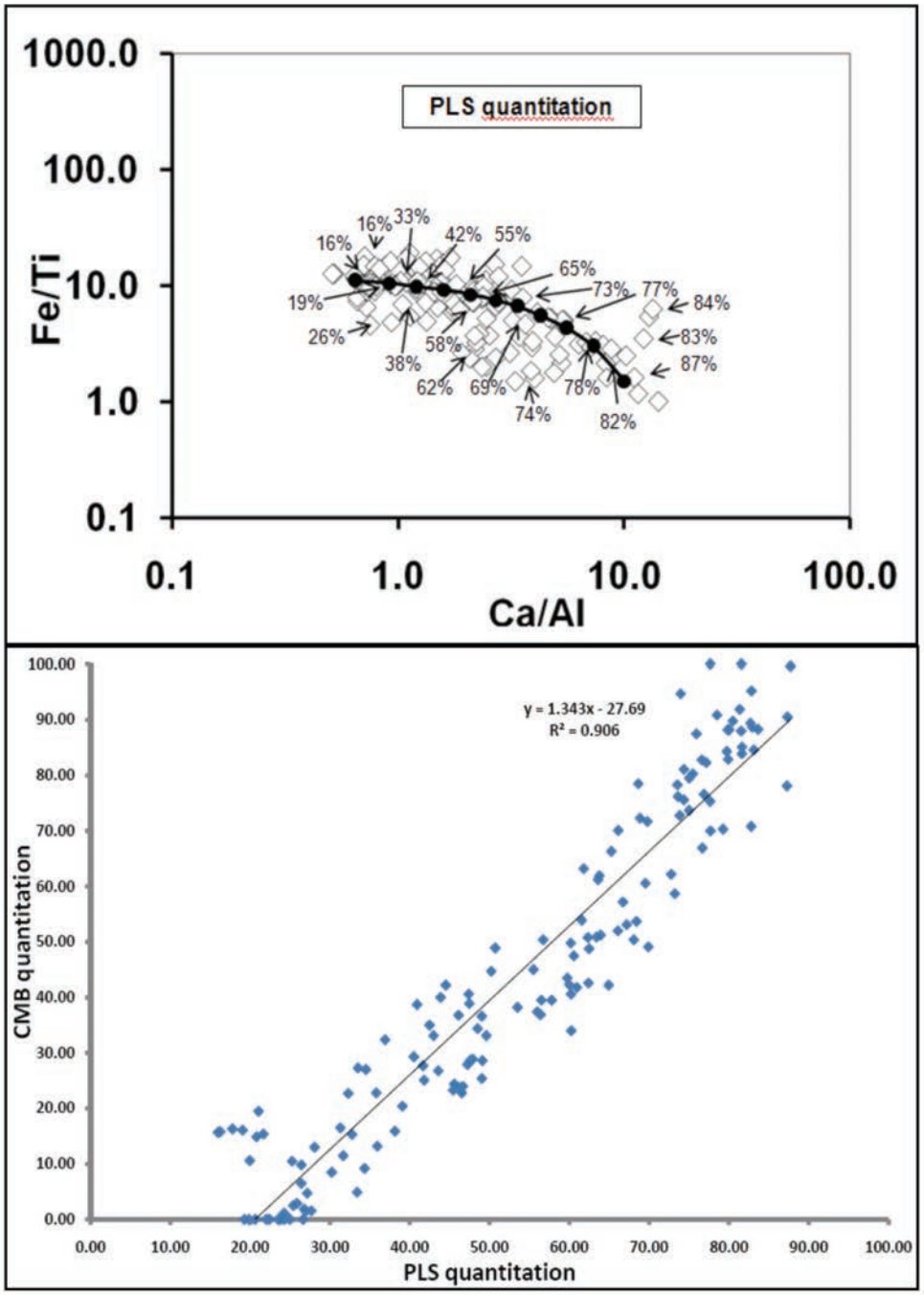

Figure 9. *Comparison between the three quantitation methods: Binary Mixing vs. Partial Least Squares (top), PLS vs. Chemical Mass Balance (bottom).*

locations usually conflicts with budgetary constraints. Geostatistical modelling such as this also provides complementary empirical data to verify theoretical dispersion modelling that is often used on and around industrial sites. In this example, the information provided has been used to inform the rationalisation of dust dispersion controls on and around the site.

Conclusions

The methods described above combine a cost-effective directional passive dust sampler with sophisticated laboratory analysis and data handling, which together offer a powerful tool for application within the non-petroleum extractive industries. The generation of fugitive dust from extractive industry sites is a widespread problem, and considerable expense is incurred in dust suppression. Even so, disputes arise on occasion between the site operator and the local community, during which it is generally assumed that all dust in the vicinity is produced by site processes.

This is rarely the case, and directional monitoring of dust emanation combined with the possibility of quantifying site dust proportion offers a significant step towards settling such disputes and away from "tick-box" surveys that are current common practice. The approach adopted here is typical of "environmental forensics" – the application of investigative environmental science to real or potential pollution events.

As is the intention of the ever-tightening legislative and regulatory regimes, it would be preferable to be proactive and to feed data generated in this way back into site planning and operational procedures, thus minimising the actual impact on the environment rather than dealing with it subsequently.

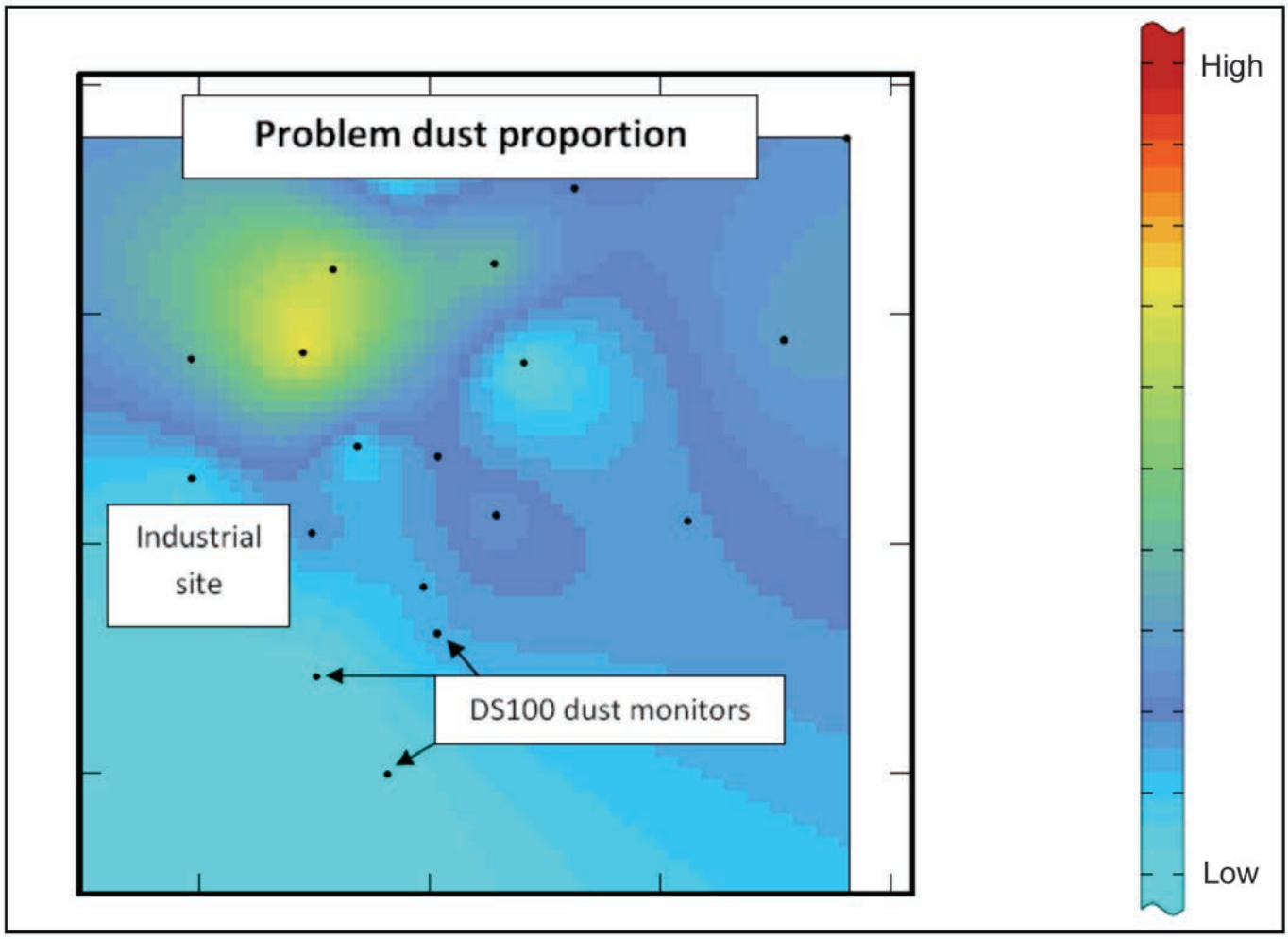

Figure 10. *An example of a fortnightly dust map generated with a combination of directional collection, chemical analysis, proportion quantitation and geostatistics.*

Acknowledgements

We are grateful to the many site operators who granted permission to use data and samples for this study, and to colleagues at DustScan and the University of Portsmouth, particularly Professor Geoffrey Walton for his encouragement and support of this work.

References

COMEAP, 2001. Statement and Report on Long-Term Effects of Particles on Mortality. Department of Health, London. The Stationery Office.

COMEAP, 2009. Report on Long-Term Effects of Particles on Mortality. Department of Health, London. Retrieved July 29 2009 from: http://www.advisorybodies.doh.gov.uk/comeap/finallongtermeffectsmort2009.htm

Datson, H. and Birch, W. J. 2006. The development of a novel method for directional dust monitoring. Environmental Monitoring and Assessment, 124, 301 – 308.

Datson , H. and Fowler, M.B. 2007. A method for the characterisation of ambient dust: geochemical analysis of directional sticky pad samples. WIT Transactions on Ecology and the Environment, 101, 413-429.

Department for Environment, Food and Rural Affairs (DEFRA), 2000. The Air Quality Strategy for England, Scotland, Wales and Northern Ireland – Working Together for Clean Air. Cm 4548, SE2000/3, NIA 7, London, The Stationery Office.

Department for Environment, Food and Rural Affairs (DEFRA), 2007. The Air Quality Strategy for England, Scotland, Wales and Northern Ireland. Cm 7169 NIA 61/06-07, London, The Stationery Office.

Environment Agency, 2004. *Monitoring of Particulate Matter in Ambient Air around Waste Facilities: Technical Guidance Document (Monitoring)* M17. Environment Agency, Bristol.

Fowler, M.B., Datson H. and Newberry, J. 2010. Quantitative assessment of dust propagation at a hazardous waste landfill: directional dust monitoring with elemental analysis. Journal of Environmental Monitoring, 12, 879-889.

The Quality of Urban Air Review Group (QUARG), 1996. *Airborne Particulate Matter in the United Kingdom: The 3rd Report of The Quality of Urban Air Review Group.* University of Birmingham, Birmingham.

Walton, G. and Datson, H. 2010. Operators can kick off the dust. Mineral Planning, 128, 16 – 17.